

PAPER • OPEN ACCESS

The application of non-destructive methods in the diagnostics of the approach pavement at the bridges

To cite this article: M Miskiewicz *et al* 2018 *IOP Conf. Ser.: Mater. Sci. Eng.* **356** 012023

View the [article online](#) for updates and enhancements.

You may also like

- [Road roughness evaluation using in-pavement strain sensors](#)
Zhiming Zhang, Fodan Deng, Ying Huang et al.
- [Evaluation of the Pavement Distress and its Impact on the Sustainability of the Traffic Operation for Selected Roads in Al-Diwaniyah City](#)
Manal Ghadban Al-Zubaidi, Hamsa Zubaidi and Bassim H. Al-Humeidawi
- [Pavement cracking measurements using 3D laser-scan images](#)
W Ouyang and B Xu

PRIME
PACIFIC RIM MEETING
ON ELECTROCHEMICAL
AND SOLID STATE SCIENCE

HONOLULU, HI
Oct 6–11, 2024

Abstract submission deadline:
April 12, 2024

Learn more and submit!

Joint Meeting of

The Electrochemical Society
•
The Electrochemical Society of Japan
•
Korea Electrochemical Society

The application of non-destructive methods in the diagnostics of the approach pavement at the bridges

M Miskiewicz, J Lachowicz, P Tysiac, P Jaskula and K Wilde

Faculty of Civil and Environmental Engineering, Gdansk University of Technology, Gdansk, Poland

Email: mikolaj.miskiewicz@pg.edu.pl

Abstract. The article presents the possibility of using non-destructive methods of road pavement diagnostics as an alternative to traditional means to assess the reasons for premature cracks adjacent to bridge objects. Two scanning methods were used: laser scanning to measure geometric surface deformation and ground penetrating radar (GPR) inspection to assess the road pavement condition. With the use of a laser scanner, an effective tool for road deformation assessment several approach pavement surfaces next to the bridges were scanned. As the result, a point cloud was obtained including spatial information about the pavement deformation. The data accuracy was about 3 mm, the deformations were presented in the form of deviation maps between the reference surface and the actual surface. Moreover characteristic pavement surface cross-sections were presented. The in situ measurements of the GPR method were performed and analysed in order to detect non-homogeneity in the density of structural layers of the pavement. Due to the analysis of the permittivity of individual layers, it was possible to detect non-homogeneity areas. The performed GPR measurements were verified by standard invasive tests carried out by drilling boreholes and taking cores from the pavement and testing the compaction and air voids content in asphalt layers.. As a result of the measurements made by both methods significant differences in layer compacting factor values were diagnosed. The factor was much smaller in the area directly next to the bridgehead and much larger in the zone located a few meters away. The research showed the occurrence of both design and erection errors as well as those related to the maintenance of engineering structures.

1. Introduction

Nowadays, non-destructive diagnostic methods are used increasingly in structural health monitoring and technical state evaluation. The possibilities of using non-invasive methods were described in [1]-[10]. The article presents road pavement [11] diagnostics of transverse cracks and surface deformation [12] adjacent to the bridge joint area of a bridge structure. The GPR scan [10] and the laser scanning technology [13]-[19] the chosen methods, the results were compared to the traditional ones performed by core drilling [20],[21]. Non-destructive diagnostic methods are commonly used [22],[23], however the novel approach is to combine them and use both. This allows a broad spectrum of inferences about the state of the analysed structure, comparable to destructive methods. Therefore this solution is able to more widely implement.



Problem description

The structure of the approach pavement has been designed and made as susceptible. Asphalt layers are laid on the base course of the unbound mixture and the subbase of the improved subgrade as a cement treated soil. In the binder course and base course, high modulus asphalt concrete (HMAC) was used. The pavement was designed for heavy traffic load. Details regarding the pavement structure are shown in Fig. 1b.

During the construction of the road nine bridge structures were built. There were two solutions for the carrying system joints. One-module leak-proof expansion joints were used, but airtight bitumen expansion joints were used as well. Two types of transition plates and their backs were designed depending on the type of a load-carrying structure applied on the back wall of the abutment. The length of the transition plates was 5 m, the thickness of them both was equal to 30 cm. The differences occurred in the shape of the transition plate fragment at the bridge joint.

In a relatively short time after the road started operating transverse cracks appeared during the first winter at the majority of expansion joints of modular bridge structures. The cracks occurred 30 cm from the steel profile of the expansion device, at the abutment of the transition plate at the bridgehead. Moreover, the cracks did not appear with bituminous expansion joints. At that time, damage was secured by flooding with a flood mass. It was a provisional only solution. No major actions were taken to remove the cracks from the moment they arose during the measurements based on documentation analysis. During the measurements it was noticed that damage was often accompanied by a visible lack of pavement surface pieces just before the cracking (Fig. 1a). In some circumstances only vertical deformation of the pavement surface appeared without cracks. Lowering the pavement surface usually occurs in the vehicle tracks, also in the areas not subjected to direct impact of the wheels, e.g. in the area of emergency lane or at the inner edges of the wings of abutments.

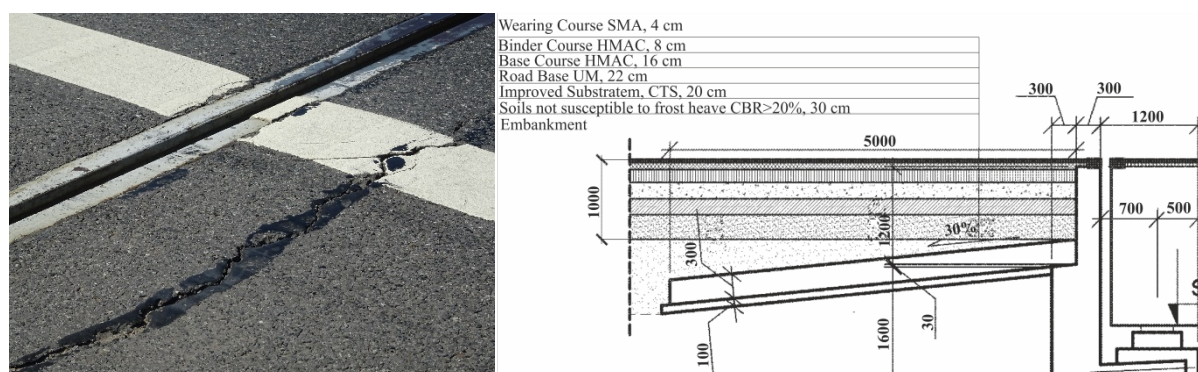


Figure 1. Analyzed detail, a) approach pavement surface condition b) pavement structure details.

2. Non-destructive testing

2.1. Ground penetrating radar method

The road surface research was carried out with the use of the IDS GPR set, including: a DAD 400 kHz control unit, a portable computer and two antennas including two transmitter-receiver pairs with 400 MHz and 900 MHz frequency. The entire system is powered by a battery. Moreover, the choice of the antenna frequency acts strongly on measurements results. The higher frequency applied, the smaller penetration depth of the electromagnetic wave is obtained, but the resolution of the radargram is higher. During the measurement mission, two antennas were used, but the paper presents the 400 MHz frequency case only, due to a greater penetration depth.

In the region of the transition bridge plate transverse and longitudinal profiles were conducted on the most-loaded lane and on the emergency lane adjacent to the bridge joint of the bridge structure. A general view with the arrangement of scanning routes on the bridge object is shown in Fig. 2.

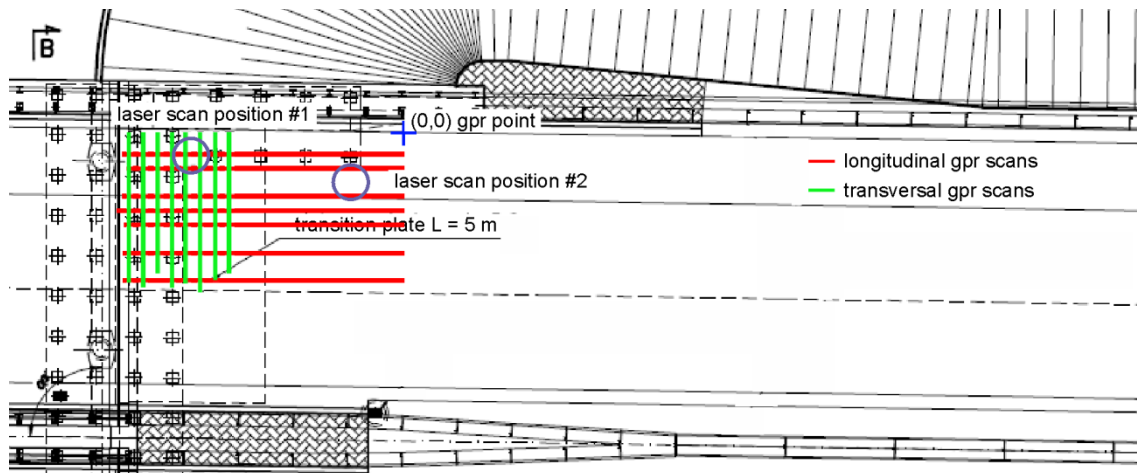


Figure 2. A general view with the arrangement of scanning routes on a bridge object and positions of the Terrestrial Laser Scanner.

Longitudinal GPR maps of the most loaded lane and the emergency lane are shown in Fig. 3 and Fig. 4a. It is worth mentioning that below each map a graph of estimated effective values of permittivity for each detected pavement structure layer is presented. Based on the thickness of successive layers and reflection times of the electromagnetic wave information, the proprietary GPR data processing algorithm estimated changes of this electrical parameter along the profile.

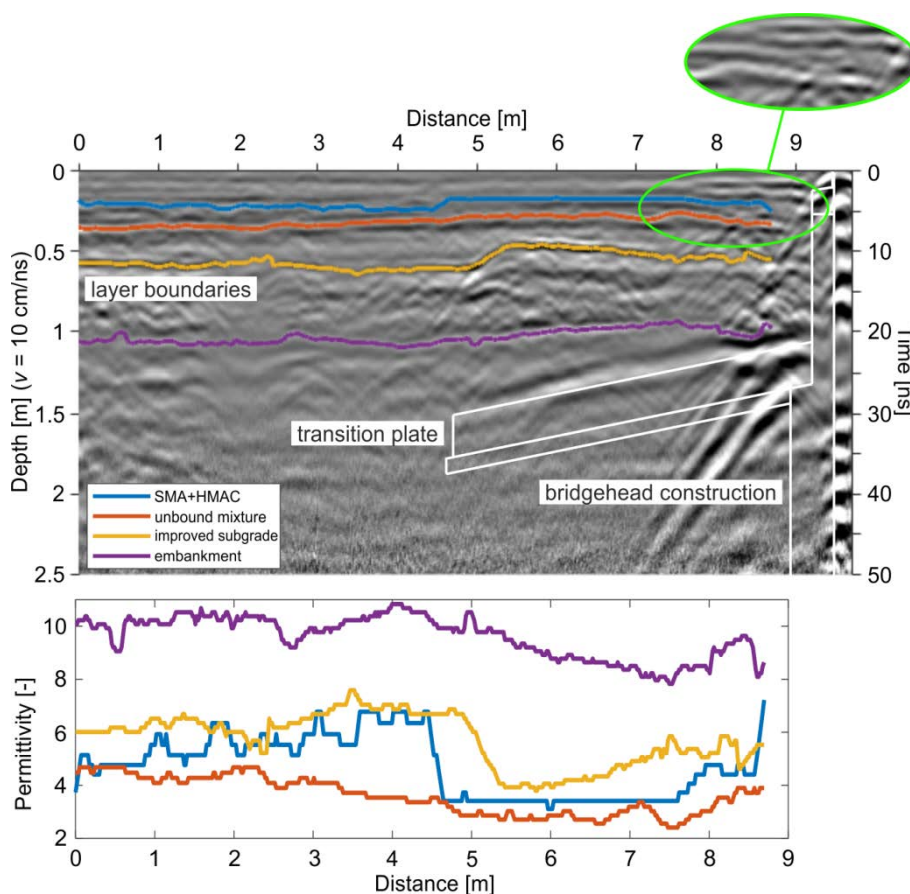


Figure 3. The slow lane (most-loaded lane) longitudinal GPR map.

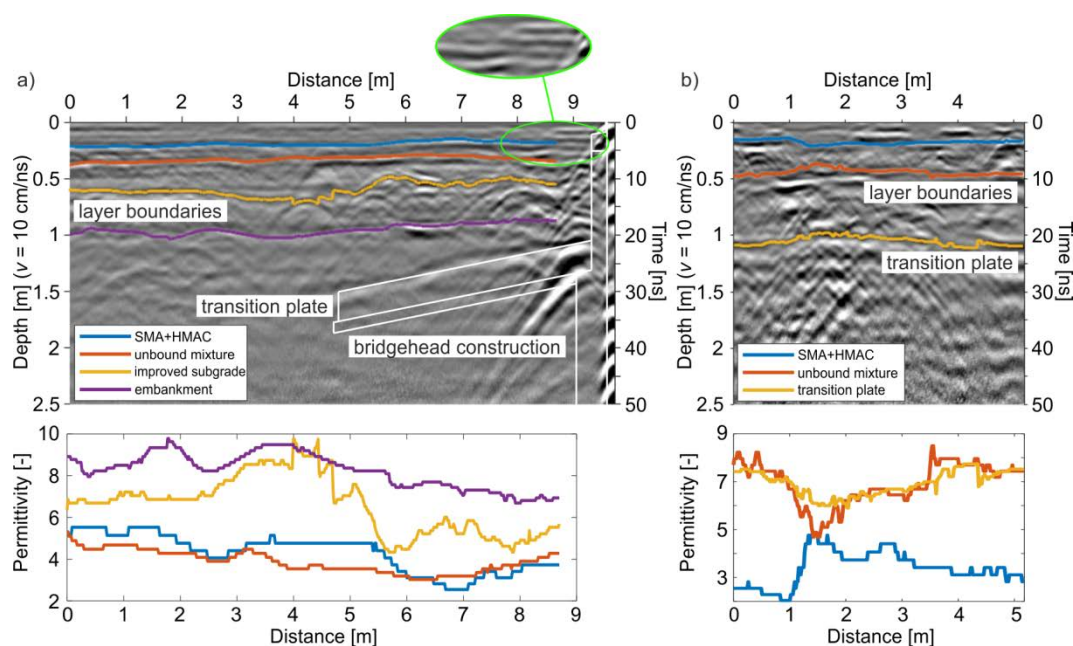


Figure 4. GPR maps a) The emergency lane longitudinal GPR map b) Transversal GPR map of approach pavement at bridge.

In addition, Table 1 lists values of the permittivity depending on the distance from the bridge joint. This parameter could be varied for one material depending on many factors including moisture and density. In the case of the analysed object it is clearly visible that the electrical permittivity changes significantly in the vicinity of the bridge joint over the transition plate, i.e. up to 4 m from the bridge joint. This may indicate areas of increased humidity or zones of inhomogeneous compaction in particular construction layers (with increased air capacity). In Table 1 these dielectric constant values are marked in red, they differ by more than 20% from the average value of a given layer.

Table 1. Effective value of the relative permittivity of the analyzed layers.
Distance from the bridge joint [m]

Lane	Layer	1	2	3	4	5	6	7
Emergency	1	3.73	3.23	2.82	4.34	4.77	4.92	4.06
	2	4.28	3.54	3.19	3.36	3.54	4.09	3.90
	3	5.53	4.94	5.69	4.71	8.38	8.74	7.18
	4	6.88	7.18	7.67	8.23	8.78	9.49	8.23
The slow lane (most-loaded)	1	4.69	3.41	3.41	3.41	6.69	5.53	5.69
	2	3.90	2.56	2.71	2.80	3.36	3.72	4.17
	3	4.74	5.19	4.25	3.98	6.69	7.15	5.83
	4	9.57	8.07	8.69	9.60	10.47	10.19	10.22

Legenda:

Layer 1 – Asphalt layers SMA +HMAC,

Layer 2 – Road base from the unbound mixture,

Layer 3 – Improved subgrade made of cement-treated soil,

Layer 4 – The top layer of the embankment.

Anomalies near the bridge joint were observed, i.e.: change of the reflected signal phase, increased reflected signal power and multiple longitudinal reflections (Fig. 3 and Fig. 4a). These anomalies may

indicate structural disturbance, increased humidity or air voids. In order to interpret the observed anomalies correctly, numerical calculations of electromagnetic wave propagation were carried out by means of the finite-difference time-domain method (FDTD). Transverse maps with permittivity diagrams are shown in Fig. 4b. It can be noticed that differences in the dielectric constant occur across the pavement, possibly caused by the low traffic load of the emergency lane.

Diagnostic tests using the GPR method showed changes in the value of permittivity of individual structural layers of the pavement in a zone around the bridge joint. Detected changes in the dielectric constant in the area of four meters from the bridge joint trigger increased porosity or humidity of the tested medium. Moreover, in case of the elevated humidity, the value of permittivity is higher than the average value due to the value of water permittivity ($\epsilon_r = 81$). However, in the case of increased porosity of the material, the permittivity value is lower than the average due to the value of air permittivity ($\epsilon_r = 1$). In conclusion, the occurrence of inhomogeneous compaction zones in the expansion zone is considered highly probable.

2.2. Laser scanning

The surface of the pavement was measured with use of the Leica P30 laser scanner. The device is capable to collect information on a scanned object at a speed of 1 million points per second with the accuracy of 2 mm at 50 meters. A huge advantage of the scanner is the noise reduction of points, at the level of 0.4 mm.

In order to process the acquired data, the ICP algorithm for scan positions alignment was used firstly. The next steps were surface extraction and noise reduction from the scan. Based on the acquired data, the most important step was the plane fitting because the reference surface of the experiment was the approximate one. After choosing points, belonging to the surface, the plane was estimated using a least-square method.

The accuracy of the point cloud resulting from scanning is equal to the approximate value of 2 mm. This refers to the accuracy of the measured distance by the scanner (1 mm by 10 m), the noise level of the point cloud (0.4 mm by 10 m) and the position alignment, where the standard deviation did not exceed 1 mm. As a result, the isometric map and cross-sections marked in Figure 5 were created.

Based on a number of the selected bridge objects, the measurements were performed on the slow lane (most-loaded lane) and on the emergency lane near the bridge joint of the bridge structure. A general view of the location of the scanner positions on the object is shown in Fig. 2. The isometric map of the scanned pavement is shown in Fig. 5. It is clearly visible that the right, more loaded lane is lowered by about 1 cm related to the reference surface. In turn, the edge of the left lane is about 1 cm above the reference position. In the immediate vicinity of the bridge joint, on the right lane zone is lowered by about 0.5 cm- 1.5 cm in relation to the reference position and by 2-3 mm in the left lane.

In addition, Fig. 6 shows cross-sections of the surface: across the carriageway in close neighborhood to the bridge joint (A-A), across the road in a section away from the bridge joint by 10m (B-B), along the right edge of the right lane (C-C). As a reference line, the points on expansion joints were taken into account in the case of cross-sections and two points at the edges of the study in the case of longitudinal sections (one on a bridge joint, the other located 10 metres away).

The cross-sections indicate a significant reduction in the right lane of the road in relation to the reference surface. In the lane adjacent to the bridge joint, the measured distance from the reference plane to the real state is on the approximately equal of 1.5 cm. On the fast lane (left lane), elevation of the pavement surface was observed in relation to the reference plane. The elevation value reaches 5 mm. In the cross-section, 10 meters away from the bridge joint, an increase in the area at the edge of the left lane was observed (1.5 cm), without noticeable changes on the right lane. In the longitudinal cross-section case, in the area of a bridge joint lowering the area was observed at the level of 1.5 cm. At a distance of about 10 m from the bridge joint the surface height oscillated near the reference values.

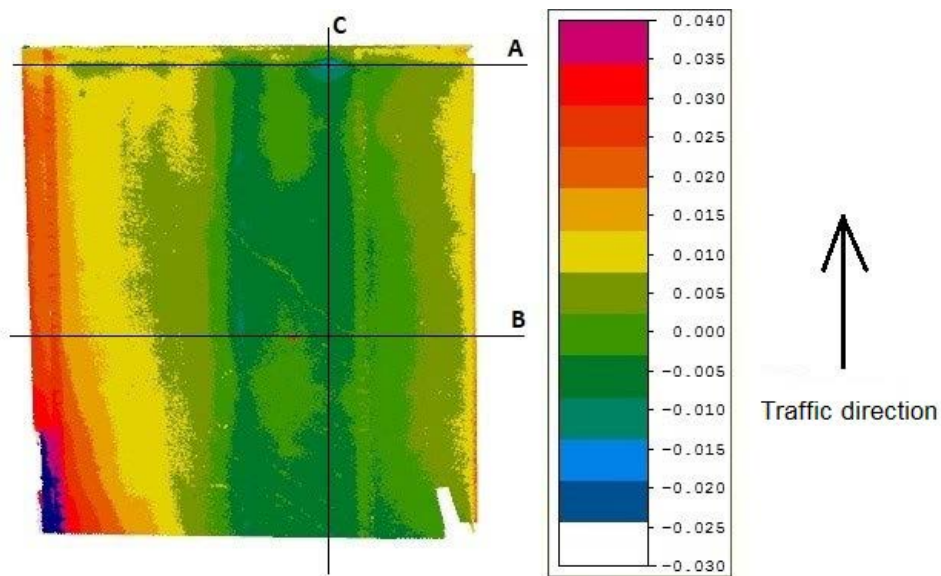


Figure 5. Isometric map of the scanned pavement surface with marked cross-sections, on the right - the distance scale between the reference surface and the real one.

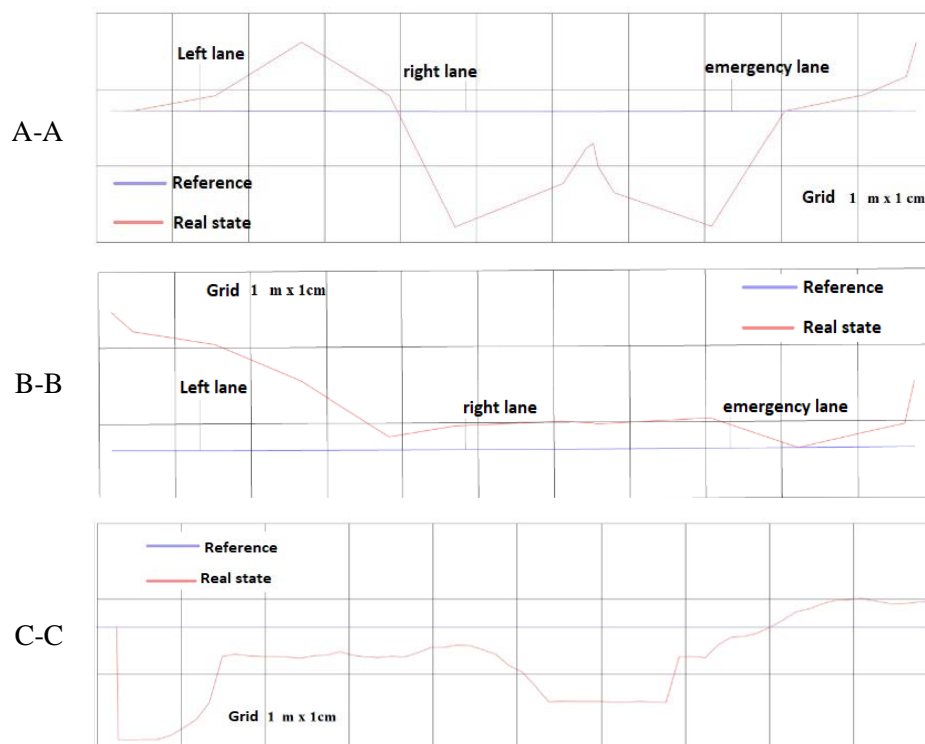


Figure 6. Cross sections of the scanned pavement (scale of 1m along the section x 1 cm after height).

The measurements show that in the close neighborhood of the bridge joint on the slow lane (most-loaded) lane there are significant deformations of the pavement surface. The maximum deformation values of the pavement in comparison to the theoretical reference level were about 1.7 cm. The recorded deformation values of the pavement indicate an uneven settlement of the surface at the entrance to the object and a resulting threshold on the edge of the wall of the outboard bridgehead.

3. Reference invasive test

In order to verify the observed zones of inhomogeneous compaction from non-destructive methods, destructive tests were performed (Fig. 7). The cores were used to determine the air void content in the asphalt layers and to determine the range of crack propagation. In addition, information on cores made it possible to determine the thickness of the each layers.

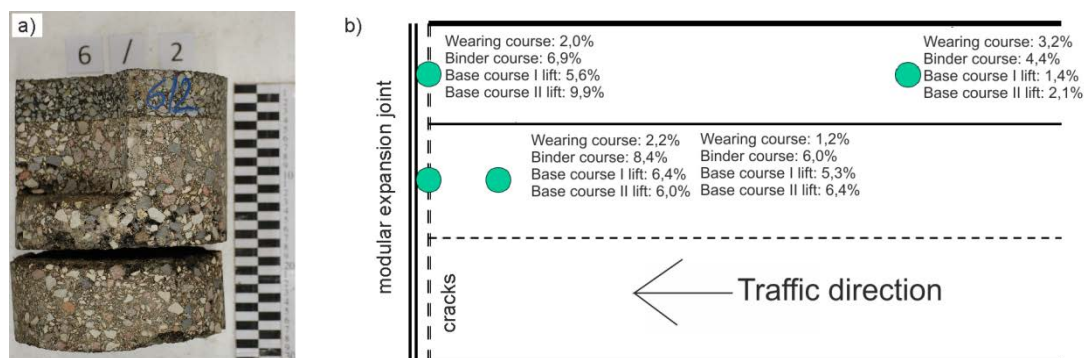


Figure 7. Invasive test results a) core picture b) results of the air voids content in the asphalt layer.

The content of the air voids in the binder course HMAC and two lift layers of the base course from HMAC in samples taken directly at joints, in the vicinity of cracks, was about 2-3 times greater than in the place located about 15 meters from the bridge joint. This would indicate a worse compaction of these layers next to the bridge, compared to the compaction on the regular section. This is confirmed by the appearance of the samples themselves. The samples taken directly at the bridge joint were heterogeneous and porous in some fragments. Tests performed in the laboratory using cores, confirmed the conclusions of non-destructive testing.

4. Conclusions

The paper presents diagnostic methods used to assess the condition of the approach pavement surface in the area of transverse cracks at the bridge joint of selected bridge objects. The measurements were performed using the GPR method and the laser scanning technology. In order to confirm the diagnosis, destructive tests were carried out.

Based on the measurements of the GPR method, as longitudinal reflections observed on radargrams, it was possible to determine relative values of electrical permeability for individual structural layers. The variations of this parameter along the scan length allowed to state that there may be zones of inhomogeneous compaction on particular layers. In addition, it can be concluded that differences in permeability values were greater for the slow lane (most-loaded lane). The collected results obtained by the terrestrial laser scanner results made a conclusion that in the close neighborhood of the bridge joint on the slow lane (most-loaded lane) significant deformations of pavement surface occur, showing the maximum pavement deformations in comparison to the theoretical reference level about 1.7 cm. The cores obtained during the destructive tests allowed to state that the air void content in the samples taken at bridge joint is much larger than in the samples taken 15 m from the bridge joint. The analysis carried out confirms that the GPR method and laser scanning technique can be successfully applied analysis to diagnose the condition of road surfaces.

This paper focuses only on presentation of the final results of research. For brevity the details of numerical simulations are omitted in this paper. These will be presented in the forthcoming papers.

References

- [1] Lachowicz J and Rucka M 2016 Experimental and Numerical Investigations for GPR Evaluation of Reinforced Concrete Footbridge *16th International Conference of Ground Penetrating Radar (GPR)* (Hong Kong) pp 1–6

- [2] Rucka M et al 2016 GPR investigation of the strengthening system of a historic masonry tower *J. Appl. Geophys.* 131 94–102
- [3] Owerko T et al Investigation of displacements of road bridges under test loads using radar interferometry - case study *Sixth International IABMAS Conference* 181-188.
- [4] Kuras P et al Advantages of radar interferometry for assessment of dynamic deformation of bridge *Sixth International IABMAS Conference* 885-891
- [5] Mazurkiewicz L et al 2017 Experimental and numerical study of steel pipe with part-wall defect reinforced with fibre glass sleeve *Int. J. of Pressure Vessels And Piping* 149 108-119
- [6] Miskiewicz M et al 2016 Structural Health Monitoring of Composite Shell Footbridge for Its Design Validation *Baltic Geodetic Congress (Geomatics) IEEE* 228-233. DOI: 10.1109/BGC.Geomatics.2016.48
- [7] Miskiewicz M et al 2017 Technical monitoring system for a new part of Gdańsk Deepwater Container Terminal *Pol. Maritime Res.* S1 (93) 24 149-155, DOI: 10.1515/pomr-2017-0033
- [8] Miskiewicz M et al 2017 Monitoring system of the road embankment *Baltic Journal of Roads and Bridge Engineering* 12 4 218-224
- [9] Chroscielewski et al 2014 Assessment of tensile forces in Sopot Forest Opera membrane by in situ measurements and iterative numerical strategy for inverse problem *Shell Structures: Theory and Applications* 3 499-502, DOI: 10.1201/b15684-125
- [10] Saarenketo T and Scullion T 2000 Road evaluation with ground penetrating radar *J. Appl. Geophys.* 43 119–38
- [11] Judycki J et al 2017 New polish catalogue of typical flexible and semi-rigid pavements *MATEC Web of Conferences* 122
- [12] Judycki J et al 2017 Field investigation of low-temperature cracking and stiffness, moduli on selected roads with conventional and high modulus asphalt concrete *Bestinfra 2017, IOP Conference Series: Materials Science and Engineering* 236, 012002
- [13] Zai D et al 2016 3D road surface extraction from mobile laser scanning point clouds, *2016 IEEE Int. Geosci. Remote Sens. Symp.* 1595–1598 DOI:10.1109/IGARSS.2016.7729407
- [14] Szulwic J and Tysiąc P 2017 Searching for road deformations using mobile laser scanning *MATEC Web of Conferences* 122 04004 DOI: 0.1051/matecconf/201712204004
- [15] Bobkowska K et al 2017 Bus bays inventory using a terrestrial laser scanning system *MATEC Web of Conferences* 122 04001 DOI: 10105104001
- [16] Janowski A et al 2016 Remote sensing and photogrammetry techniques in diagnostics of concrete structures *Comput. Concr.* 18 3 405–420
- [17] Janowski A et al 2015 Airborne and mobile laser scanning in measurements of sea cliffs on The Southern Baltic *15th Multidisciplinary Scientific GeoConference SGEM 2015, Vol 2*
- [18] Nagrodzka-Godycka K et al 2014 The method of analysis of damage reinforced concrete beams using terrestrial laser scanning *14th SGEM GeoConference on Informatics, Geoinformatics and Remote Sensing* 3 335-342
- [19] Janowski A et al 2014 Modes of Failure Analysis in Reinforced Concrete Beam Using Laser Scanning and Synchro-Photogrammetry. How to apply optical technologies in the diagnosis of reinforced concrete elements? *Second Int. Con. on Advances in Civil, Structural and Environmental Engineering - ACSEE 2014* 16-20
- [20] Judycki J et al 2015 Investigation of low-temperature cracking in newly constructed high modulus asphalt concrete base course of a motorway pavement *Journal of Road Materials and Pavement Design* 16 362-388 DOI:10.1080/14680629.2015.1029674
- [21] Judycki J and Jaskula P 2010 Diagnostyka i modernizacja konstrukcji nawierzchni drogowych *Autostrady* 12/2010 24-31
- [22] Graczyk M et al 2014 Zastosowanie georadaru w diagnostyce stanu konstrukcji nawierzchni i ocenie bezpieczeństwa eksploatacyjnego lotnisk *Logistyka* 3 2128–39
- [23] Krysiński L and Sudyka J 2013 GPR abilities in investigation of the pavement transversal cracks *J. Appl. Geophys.* 97 27–36